The Inflation Uncertainty-Inflation Relationship: Time Variation Across Latin America and the G7

Mauricio Alvarado and Gabriel Rodríguez

Department of Economics
Pontificia Universidad Católica del Perú

XLIII Encuentro de Economistas
Pontificia Universidad Católica del Perú
Oct 22nd, 2025

Contents

Motivation

- Uncertainty: Conditional volatility of a disturbance that is unforecastable from the perspective of economic agents (Jurado et al., 2015);
- Inflation Uncertainty: Conditional volatility of future inflation around its expected path;
  - It is relevant for Central banks because higher uncertainty hampers expectation-forming and may prompt them to adjust interest rate settings and communication to reanchor inflation expectations;
- There is broad consensus that high uncertainty about inflation expectations complicates monetary policy and raises costs for market participants (Friedman, 1977; Ball, 1992; Golob, 1994);
- Understanding the relationship between inflation (y_t) and inflation uncertainty (h_t) is essential, as both factors play a central role in policy design;

Motivation

- The literature identifies two main views:
  1. Friedman (1977) argues that higher inflation leads to greater inflation uncertainty
     $$y_t \rightarrow h_t$$
  2. Cukierman and Meltzer (1986) claim that rising inflation uncertainty drives inflation upward
     $$h_t \rightarrow y_t$$
- Nevertheless, studies in advanced economies offer mixed evidence for both views. Evidence from Latin America, although less extensive, supports Friedman's view.

Objectives

- This study examines the evolving relationship between inflation uncertainty and inflation for:
  - Seven Latin American countries (Brazil, Chile, Colombia, Ecuador, Mexico, Peru, and Uruguay)
  - The G7 (Canada, France, Germany, Italy, Japan, the UK, and the US)
- Comparing both group of countries and analyzing the dynamics of their inflation uncertainty-inflation relationship during recessions, hyperinflation episodes, and pre- and post-IT adoption periods;
- The analysis centers on the Cukierman-Meltzer hypothesis, adopting a time-varying perspective.

Literature

- Friedman (1977):
  - When overall price levels rises, agents find it increasingly difficult to anticipate future inflationary trends and macroeconomic conditions.
  - This uncertainty undermines the ability of plan and make informed decisions about consumption, investment, and wage setting.
- Cukierman and Meltzer (1986):
  - There is ambiguity about the exact timing for a Central bank to adopt policies aimed at reducing inflation.
  - A credible central bank can implement unanticipated policies during periods of high inflation uncertainty to alter expectations and leverage the trade-off between inflation and unemployment, resulting in a positive uncertainty-inflation relationship.
- Following the same causality direction of Cukierman and Meltzer (1986), but with a negative sign, is the Holland (1995) hypothesis:
  - A negative uncertainty-inflation relationship suggest that if policymakers view inflation uncertainty as costly, they have strong incentives to implement policies to control inflation.

Friedman (1977)'s support

- First attemps (limited empirical support); see Engle (1982) and Bollerslev (1986) using ARCH and GARCH models.
- Advanced Economies; see Brunner and Hess (1993), Grier and Perry (1998), Kontonikas (2004), Berument and Dincer (2005), and Daal et al. (2005).
- Emerging Economies; see Grier and Grier (1998), Magendzo (1998), Carvalheiro (1999), Fernández Valdovinos (2000), Daal et al. (2005), Bojanic (2013), and Solera (2003).

Cukierman and Meltzer (1986)'s support

- Advanced Economies; see Crawford and Kasumovich (1996), Grier and Perry (1998), Daal et al. (2005), Berument et al. (2009), Chan (2017), and Hou (2020).
- OECD Countries; see Le (2023).
- Emerging Economies; see Daal et al. (2005), Thornton (2007), Ferreira and Palma (2017), and Varlik et al. (2017).

Holland (1995)'s support

- Advanced Economies; see Grier and Perry (1998), Berument and Dincer (2005), and Balcilar and Ozdemir (2013).
- Emerging Economies; see Daal et al. (2005), and Thornton (2007).

The TVP-SVM-TVMI Model (Hou, 2020)

Based on Hou (2020), as an extension of the TVP-SVM model of Chan (2017), with time-varying mixture innovations:

$$y_t = \tau_t + \alpha_t e^{h_t} + \epsilon_t^y, \qquad \epsilon_t^y \sim \mathcal{N}\left(0, e^{h_t}\right),$$

where:

$$\begin{aligned}
h_t &= h_{t-1} + \epsilon_t^h, & \epsilon_t^h &\sim \mathcal{N}\left(0, \sigma_h^2\right), \\
\gamma_t &= (\alpha_t, \tau_t)', & & \\
\gamma_t &= \gamma_{t-1} + \epsilon_t^\gamma, & \epsilon_t^\gamma &\sim \mathcal{N}\left(\mathbf{0}, \mathbf{\Sigma}\right), \\
\mathbf{\Sigma} &= \begin{bmatrix} \sigma_\alpha^2 & 0 \\ & \sigma_\tau^2 \end{bmatrix} & & \\
\alpha_t &= \alpha_{t-1} + \epsilon_t^\alpha, & \epsilon_t^\alpha &\sim \mathcal{N}\left(0, \sigma_{K_t}^2\right), \\
\tau_t &= \tau_{t-1} + \epsilon_t^\tau, & \epsilon_t^\tau &\sim \mathcal{N}\left(0, \sigma_\tau^2\right).
\end{aligned}$$

- $K_t \in \{0, 1\}$ denotes the states of the variance for α_t's innovation
- The distribution of $\sigma_{K_t}^2$ is defined as $\left(\sigma_0^2, \sigma_1^2\right) \sim \left(\mathcal{IG}\left(\nu_0, S_0\right) \times \mathcal{IG}\left(\nu_1, S_1\right)\right) \mathbb{1}\left(\sigma_0^2 < \sigma_1^2\right)$
- When $K_t = 1$, the variance of the innovation ϵ_t^α experience a level shift and changes to σ_1^2 with a time varying mixture probability of $\Pr\left(K_t = 1 \mid \pi_t\right) = \pi_t$
- We adopt the qualitative convention that a structural break occurs whenever π_t exceeds 50%

A (Restricted) Model

Hou's (2020) TVP-SVM-TVMI model has several differences from Chan's (2017) TVP-SVM model. To ensure comparability between the two models, we used a restricted TVP-SVM model. The restrictions are removed in the Alternative Results section.

The restricted TVP-SVM model is defined as:

$$y_t = \tau_t + \alpha_t e^{h_t} + \epsilon_t^y, \qquad \epsilon_t^y \sim \mathcal{N}\left(0, e^{h_t}\right),$$

where:

$$\begin{aligned}
h_t &= h_{t-1} + \epsilon_t^h, & \epsilon_t^h &\sim \mathcal{N}\left(0, \sigma_h^2\right), \\
\gamma_t &= (\alpha_t, \tau_t)', \\
\gamma_t &= \gamma_{t-1} + \epsilon_t^\gamma, & \epsilon_t^\gamma &\sim \mathcal{N}\left(\mathbf{0}, \mathbf{\Sigma}\right), \\
\mathbf{\Sigma} &= \begin{bmatrix} \sigma_\alpha^2 & 0 \\ & \sigma_\tau^2 \end{bmatrix} \\
\alpha_t &= \alpha_{t-1} + \epsilon_t^\alpha, & \epsilon_t^\alpha &\sim \mathcal{N}\left(0, \sigma_\alpha^2\right), \\
\tau_t &= \tau_{t-1} + \epsilon_t^\tau, & \epsilon_t^\tau &\sim \mathcal{N}\left(0, \sigma_\tau^2\right).
\end{aligned}$$

- Only the time-varying Cukierman-Meltzer (1986) hypotheses can be tested using α_t

Estimation Algoithm (Gibbs Sampling)

Each block of parameters is estimated separately conditioned to the update of the other blocks. Using the approach of Chan and Strachan (2014), Chan (2017) and Hou (2020), based on precision sampling of Chan and Jeliazkov (2009):

1. Draws from $p\left(\mathbf{h} \mid \boldsymbol{\tau}, \boldsymbol{\alpha}, \sigma_h^2, \boldsymbol{y}\right)$;
2. Draws from $p\left(\boldsymbol{\tau}, \boldsymbol{\alpha} \mid \mathbf{h}, \sigma_\tau^2, \mathbf{K}, \sigma_0^2, \sigma_1^2, \boldsymbol{y}\right)$;
3. Draws from $p\left(\sigma_\tau^2 \mid \boldsymbol{\tau}\right)$;
4. Draws from $p\left(\sigma_h^2 \mid \mathbf{h}\right)$;
5. Draws from $p\left(\mathbf{K} \mid \boldsymbol{\alpha}, \boldsymbol{\pi}\right) = \prod_{t=1}^{T} p\left(K_t, \boldsymbol{\alpha}, \pi_t\right)$;
6. Draws from $p\left(\boldsymbol{\pi} \mid \mathbf{K}\right) = \prod_{t=1}^{T} p\left(\pi_t, K_t\right)$;
7. Draws from $p\left(\sigma_0^2, \sigma_1^2 \mid \boldsymbol{\alpha}, \mathbf{K}\right)$;
8. Previous (1) to (7) steps are repeated N times.

Further details are found in Section 4 and Appendix A of Hou (2020).

Computing Marginal Log-Likelihood

- Hou (2020) uses a log-marginal likelihood (LogML) based on a predictive likelihood approach.
- For a given model M_i, the marginal likelihood is defined as:

$$p\left(\boldsymbol{y}|M_i\right) = \int p\left(\boldsymbol{y} \mid \boldsymbol{\theta}_i, M_i\right) p\left(\boldsymbol{\theta}_i \mid M_i\right) d\boldsymbol{\theta}_i,$$

  where $\boldsymbol{\theta}_i$ is the parameter vector of the model M_i.
- The marginal likelihood is represented as the product of one-step-ahead predictive likelihoods evaluated at each data point:

$$p\left(\boldsymbol{y}|M_i\right) = p\left(y_1 \mid M_i\right) \prod_{t=2}^{T} p\left(y_t \mid y_1, ..., y_{t-1}, M_i\right).$$

- Calculate the Bayes Factor: $\mathrm{BF}_{i,j} = \frac{p(\boldsymbol{y}|M_i)}{p\left(\boldsymbol{y}|M_j\right)}$. We prefer M_i, BF times than the M_j.

Data

- Annualized quarterly inflation rates:
$$y_t = 400 \times \left(\log CPI_t - \log CPI_{t-1} \right).$$
- Countries:
  - Latin America: Brazil, Chile, Colombia, Ecuador, Mexico, Peru and Uruguay
  - G7: Canada, France, Germany, Italy, Japan, the UK and the US
- Source: International Financial Statistics (IFS), except for the US, with was obtained from the Federal Reserve Economic Data (FRED) repository.
- Horizon:
  - Q1 1948 to Q4 2023 ($T = 304$): US and Canada
  - Q2 1955 to Q4 2023 ($T = 275$): Colombia, France, Germany, Italy, Japan, and the UK
  - Q2 1957 to Q4 2023 ($T = 267$): Ecuador, Mexico, Peru and Uruguay
  - Q2 1970 to Q4 2023 ($T = 215$): Chile
  - Q1 1980 to Q4 2023 ($T = 176$): Brazil

Data

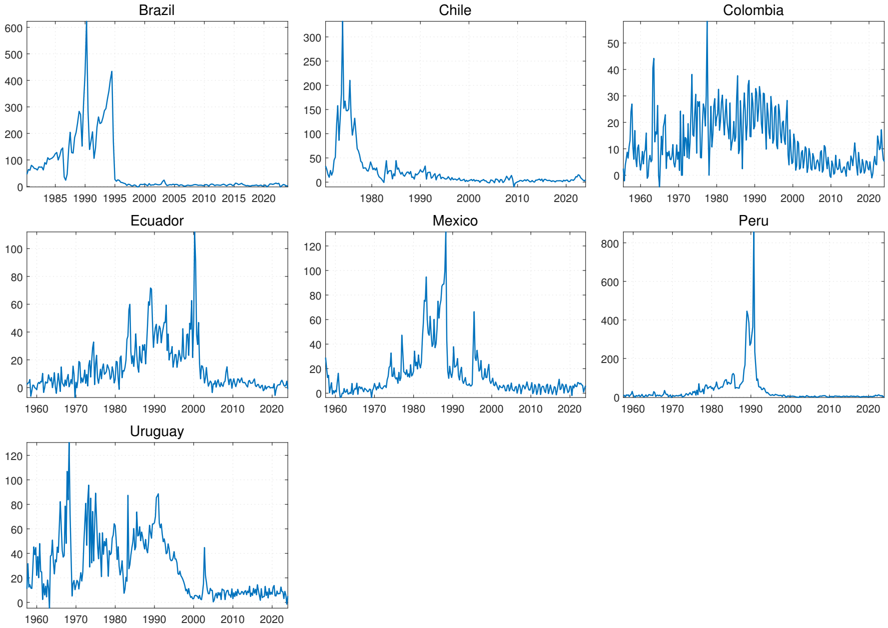

Figure: Latin America: Time Series. Sample 1948Q1-2023Q4

Data

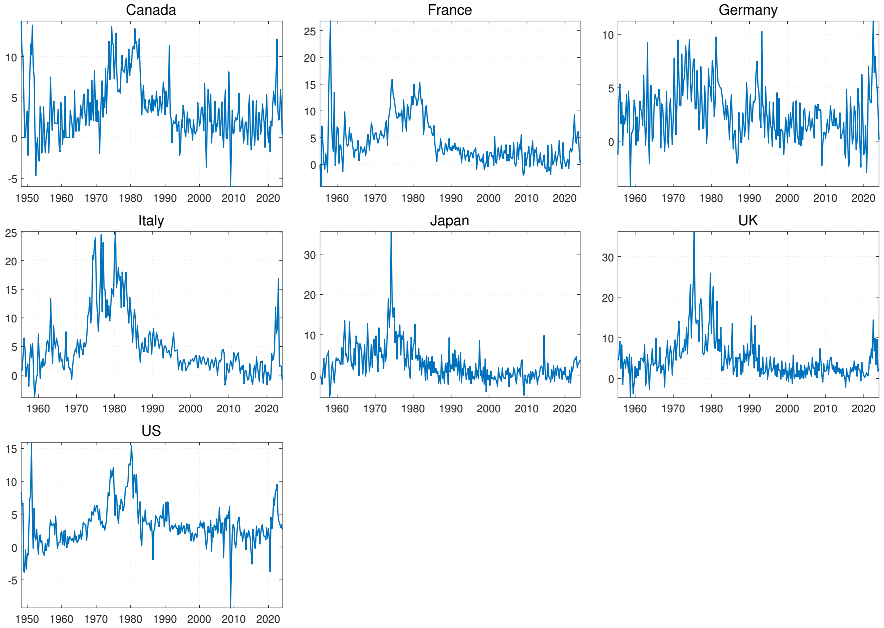

Figure: G7: Time Series. Sample 1948Q1-2023Q4

Priors for the hyperparameters are small and relative non-informative in both models:

- $\mu \sim \mathcal{N}(\mu_0, V_\mu)$, $\phi \sim \mathcal{N}(\phi_0, V_\phi)\mathbb{1}(|\phi| < 1)$, $\beta \sim \mathcal{N}(\beta_0, V_\beta)$, $\sigma_h^2 \sim \mathcal{IG}(\nu_{\sigma^2}, S_{\sigma^2})$, $\mathbf{\Sigma} \sim \mathcal{IW}(\nu_{\mathbf{\Sigma}}, S_{\mathbf{\Sigma}})$;
- $(\sigma_0^2, \sigma_1^2) \sim (\mathcal{IG}(\nu_0, S_0) \times \mathcal{IG}(\nu_1, S_1))\mathbb{1}(\sigma_0^2 < \sigma_1^2)$;
- $\Pr(K_t = 1|\pi_t) = \pi_t$, $\pi_t \sim \mathcal{B}(p_{1,t}, p_{2,t})$;
- $\nu_{\sigma^2} = \nu_{\mathbf{\Sigma}} = 10$, $S_{\sigma^2} = 0.36$ and $S_{\mathbf{\Sigma}} = diag(0.5625, 0.09)$ that imply that $\mathbb{E}(\sigma_h^2) = 0.2^2$, $\mathbb{E}(\sigma_\alpha^2) = 0.1^2$, $\mathbb{E}(\sigma_\tau^2) = 0.25^2$, and $\mathbb{E}(\sigma_{\alpha,\tau}) = 0$;
- $\nu_0 = \nu_1 = 10$, $S_0 = 0.09$, $S_1 = 90$, and $p_{1,t} = 1$ and $p_{2,t} = 99$ that imply that $\mathbb{E}(\pi_t) = 0.01$.

Selection of Models

- 55,000 simulation; burning first 5,000. Result: 50,000 posterior draws used to calculate the LogML;
- The TVP-SVM-TVMI and the Restricted version models are compared with an unobserved components (UC) model—a special case of the model where $\alpha_t = 0$; i.e., there is no uncertainty-inflation relationship;
- TVP-SVM-TVMI model is favored for Brazil, Mexico, Uruguay, Canada, France, and the US; i.e., 6 out of 14 countries;
- The Restricted version model is preferred for Chile, Colombia, Ecuador, Peru, Germany, Italy, Japan, and the UK; i.e., 8 out of 14 countries;
- For the latter group, the LogML criterion provides evidence supporting the presence of structural breaks in the uncertainty-inflation dynamics.

Table: Log-Marginal Likelihood (LogML)

	UC Model	Restricted Version Model	TVP-SVM-TVMI Model
		(A) Latin America	
Brazil	-741.034	-646.590	**-638.513**
Chile	-751.809	**-678.405**	-678.667
Colombia	-938.790	**-923.970**	-926.362
Ecuador	-923.208	**-869.012**	-870.981
Mexico	-917.133	-836.434	**-835.630**
Peru	-974.009	**-887.579**	-888.003
Uruguay	-1039.058	-967.495	**-965.591**
		(B) G7	
Canada	-729.298	-715.767	**-715.574**
France	-608.404	-589.790	**-589.106**
Germany	-616.772	**-614.920**	-617.144
Italy	-640.138	**-609.505**	-610.074
Japan	-701.406	**-693.126**	-695.743
UK	-725.241	**-705.649**	-707.884
US	-639.013	-618.746	**-617.509**

For each model we obtain a total of 50,000 posterior draws after a burn-in period of 5,000. The LogML is obtained from the one step ahead predictive likelihoods evaluated at the observed data, following Hou (2020). Bold values are the highest LogML between the models.

Estimated Posterior Parameters

- The mean of σ_h^2 is higher in Latin American countries compared to the G7, reflecting the higher volatility associated with hyperinflation episodes and the increased magnitude of h shocks in the former group;
- The mean of σ_1^2 substantially exceeds that of σ_0^2 across all countries in the TVP-SVM-TVMI model, consistent with its role in modeling drastic changes in the dynamics of α_t.

Table: Five Quarters with Highest Probabilities of Break Occurrence in α_t

	1°	2°	3°	4°	5°
	(A) Latin America				
Brazil	**1994Q4 (1.000)**	**1987Q1 (0.782)**	**1986Q2 (0.767)**	1994Q3 (0.068)	2022Q3 (0.043)
Chile	2009Q1 (0.180)	2021Q4 (0.089)	2013Q3 (0.060)	2021Q3 (0.047)	1984Q4 (0.046)
Colombia	2022Q1 (0.100)	1963Q1 (0.030)	1963Q3 (0.016)	2021Q1 (0.012)	1998Q3 (0.010)
Ecuador	2015Q3 (0.072)	2021Q1 (0.036)	1958Q2 (0.024)	2020Q3 (0.023)	2015Q4 (0.022)
Mexico	**1988Q2 (0.813)**	**1976Q4 (0.692)**	1995Q1 (0.496)	1995Q3 (0.183)	1958Q2 (0.118)
Peru	**1990Q4 (0.686)**	1990Q3 (0.495)	1978Q1 (0.157)	1985Q4 (0.045)	1976Q3 (0.040)
Uruguay	**1983Q1 (0.993)**	**1983Q2 (0.958)**	**2002Q3 (0.712)**	**2002Q4 (0.618)**	1998Q4 (0.195)
	(B) G7				
Canada	**1991Q2 (0.673)**	1952Q1 (0.105)	1973Q2 (0.097)	1973Q1 (0.089)	1991Q1 (0.079)
France	**1985Q3 (0.708)**	1967Q4 (0.159)	1957Q3 (0.099)	1985Q4 (0.092)	1961Q4 (0.091)
Germany	2021Q1 (0.092)	2008Q4 (0.086)	1985Q3 (0.021)	2008Q3 (0.014)	1985Q2 (0.011)
Italy	1996Q3 (0.263)	2023Q1 (0.234)	2008Q4 (0.158)	1959Q4 (0.068)	2021Q1 (0.058)
Japan	2022Q1 (0.125)	2021Q3 (0.094)	2022Q2 (0.055)	2008Q4 (0.030)	2021Q4 (0.023)
UK	2021Q2 (0.022)	2023Q3 (0.008)	2021Q4 (0.008)	1956Q3 (0.008)	1982Q3 (0.007)
US	2008Q4 (0.444)	1981Q4 (0.422)	1948Q4 (0.401)	2020Q3 (0.383)	2021Q2 (0.308)

The quarters are ranked from 1st to 5th based on their posterior probability of a break occurrence in the uncertainty-inflation relationship α_t (in parentheses), also denoted as $\Pr(K_t = 1|\pi_t) = \pi_t$. The probability π_t is estimated using the TVP-SVM-TVMI model. Dates in bold are those that have a probability greater than 50%.

Dynamics of h_t

- The dynamics of h_t are similar across both models, with slight differences due to the structural breaks in α_t within the TVP-SVM-TVMI model;
- Latin American economies have generally faced higher inflation uncertainty compared to the G7, particularly during the 1980s "lost decade," characterized by fiscal imbalances, excessive money creation, rising external debt, shortages of essential goods, and currency depreciation;
- Although inflation remained high in Brazil, Colombia, Ecuador, Peru, and Uruguay during the early 1990s, inflation uncertainty significantly declined at the onset of the new millennium, coinciding with IT adoption in many Latin American countries (Broto, 2011);
- Three common scenarios of high inflation uncertainty emerge among Latin American and G7 countries: (i) the Great Inflation of the 1970s; (ii) the global recession during the GFC in 2008-2009; and (iii) in 2022, by adverse impacts on hydrocarbon and fertilizer prices due to the Russia-Ukraine conflict.

Dynamics of α_t

- We also use the dynamic probability test of $\alpha_t \neq 0$, following Koop et al. (2010). This test is defined by $\Pr(\alpha_t \neq 0|\boldsymbol{y}) = 1/(1 + \mathrm{PO}_t)$, where PO_t is the posterior odds ratio favoring the hypothesis $\alpha_t = 0$, calculated using the Savage-Dickey density ratio: $\mathrm{PO}_t = \frac{p(\alpha_t=0|\boldsymbol{y})}{p(\alpha_t=0)}$. A probability exceeding 50% indicates statistical significance for the α_t component in the Restricted model;
- Across both models, α_t remains positive and statistically significant during periods of elevated inflation uncertainty. This supports the Cukierman-Meltzer hypothesis (1986), which posits that monetary authorities can deploy surprise policies under high uncertainty to dampen inflation expectations, thereby capitalizing on this positive correlation;
- The TVP-SVM-TVMI model reveals ten structural breaks in α_t among Latin American countries and two in G7 economies, highlighting the sharper volatility experienced by the former group during hyperinflation episodes;
- In contrast, significant changes in the G7 do not generally meet the threshold for structural breaks, as their probabilities fall below 50%.

Dynamics of h_t and α_t for Brazil, Mexico and Peru

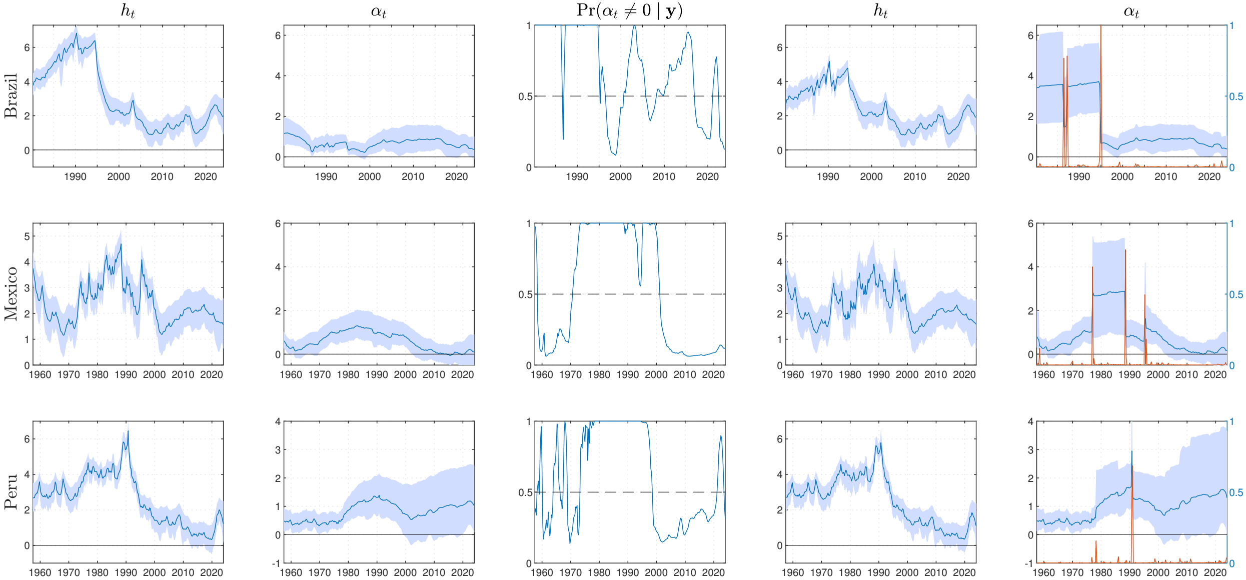

Figure: The Evolution of h_t (1st column) and α_t (2nd column), and the Dynamic Posterior Probabilities of $\alpha_t \neq 0$ (3rd column) for the Restricted Model. The Evolution of h_t (4th column), and α_t and its Probabilities of Break Occurrence $\Pr(K_t = 1|\pi_t) = \pi_t$ (red line) (5th column) for the TVP-SVM-TVMI Model. The blue lines are Median Values. The sky-blue areas are 5- and 95-percentiles Bands.

Dynamics of h_t and α_t for Canada, Germany and the US

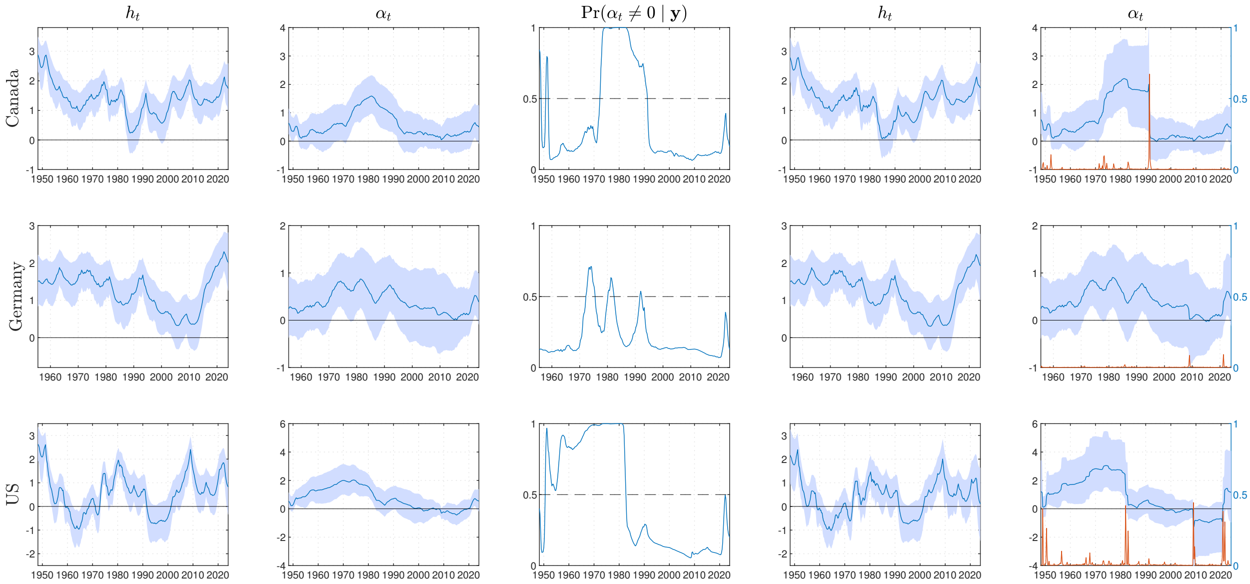

Figure: The Evolution of h_t (1st column) and α_t (2nd column), and the Dynamic Posterior Probabilities of $\alpha_t \neq 0$ (3rd column) for the Restricted Model. The Evolution of h_t (4th column), and α_t and its Probabilities of Break Occurrence $\Pr(K_t = 1|\pi_t) = \pi_t$ (red line) (5th column) for the TVP-SVM-TVMI Model. The blue lines are Median Values. The sky-blue areas are 5- and 95-percentiles Bands.

Based on Chan (2017):

$$y_t = \tau_t + \alpha_t e^{h_t} + \epsilon_t^y, \qquad \epsilon_t^y \sim \mathcal{N}\left(0, e^{h_t}\right),$$

where:

$$\begin{aligned}
h_t &= \mu + \phi\left(h_{t-1} - \mu\right) + \beta y_{t-1} + \epsilon_t^h, \qquad \epsilon_t^h \sim \mathcal{N}\left(0, \sigma_h^2\right), \\
\gamma_t &= \left(\alpha_t, \tau_t\right)', \\
\gamma_t &= \gamma_{t-1} + \epsilon_t^\gamma, \qquad \epsilon_t^\gamma \sim \mathcal{N}\left(\mathbf{0}, \mathbf{\Sigma}\right), \\
\mathbf{\Sigma} &= \begin{bmatrix} \sigma_\alpha^2 & \sigma_{\alpha,\tau} \\ & \sigma_\tau^2 \end{bmatrix}.
\end{aligned}$$

- Friedman (1977) hypotheses can be tested using β
- Time-varying Cukierman-Meltzer (1986) hypotheses can be tested using α_t
- To obtain the posterior parameters of the TVP-SVM model, steps (5) and (6) are omitted, and in step (7), the parameter σ_α^2 is sampled instead of $\left(\sigma_0^2, \sigma_1^2\right)$.

Alternative Results: The TVP-SVM Model of Chan (2017)

- This section revisits the estimation of the TVP-SVM model from Chan (2017) without the constraints $\mu = 0$, $\phi = 1$, $\beta = 0$, and $\sigma_{\alpha,\tau} = 0$;
- Relaxing these restrictions provides additional insights into the posterior parameter statistics. The priors used in this estimation follow Chan (2017): $\mu_0 = 0$, $\mathbb{V}(\mu_0) = 10$, $\phi_0 = 0.97$, $\mathbb{V}(\phi_0) = 0.1^2$, $\beta_0 = 0$, and $\mathbb{V}(\beta_0) = 10$. Additionally, for $\sigma^2 \sim \mathcal{IG}(\nu_{\sigma^2}, S_{\sigma^2})$ and $\mathbf{\Omega} \sim \mathcal{IW}(\nu_\Omega, S_\Omega)$, uninformative priors with low degrees of freedom are assumed: $\nu_{\sigma^2} = \nu_\Omega = 10$, with scale parameters $S_{\sigma^2} = 0.36$ and $S_\Omega = diag(0.13, 0.8125)$;
- β is not statistically significant for any country, as its credible intervals include zero. This suggests that Friedman's hypothesis does not hold in any of the cases analyzed;
- To assess the persistence of log-inflation uncertainty h_t, the analysis examines ϕ using the half-life shock (HLS) metric. The findings indicate that inflation uncertainty shocks are more persistent in Latin America than in the G7, meaning that AEs recover more quickly from uncertainty shocks than EMEs;
- The results also indicate that $\sigma_{\alpha,\tau}$ is not statistically significant for any country, suggesting no evidence that long-run inflation (τ_t) is correlated with the transitory effects of inflation uncertainty on inflation (α_t).

Conclusions

The main findings are as follows.

1. The Restricted model is preferred over the TVP-SVM-TVMI model in 8 out of 14 countries;
2. Latin America has experienced greater inflation uncertainty than the G7, particularly during the 1980s—the so-called "lost decade";
3. Inflation uncertainty is significantly more persistent in Latin America than in the G7, according to the alternative estimates of ϕ;
4. There is no evidence that the hypothesis of Friedman (1977) holds for any of the countries, based on the alternative estimates of β;
5. In contrast, the hypothesis of Cukierman and Meltzer (1986) holds, as the uncertainty-inflation relationship is positive and time-varying in all countries;
6. This relationship is stronger and statistically significant during periods of high inflation uncertainty;
7. There is greater evidence of structural breaks in the uncertainty-inflation relationship in Latin America—likely due to its history of hyperinflation episodes—than in the G7.

Policy Implications

- During periods of high inflation uncertainty, monetary authorities may leverage the positive inflation-uncertainty relationship to implement surprise policies geared toward lowering inflation expectations;
- A sharp decline in inflation expectations due to an unexpected policy intervention could lead to a significant drop in current inflation, consistent with Cukierman and Meltzer (1986);
- In contrast, there is no evidence supporting the hypothesis of Friedman (1977), which posits that inflation is purely a monetary phenomenon with no direct link to inflation uncertainty.

Appendix

Dynamics of h_t and α_t for Chile, Colombia and Ecuador

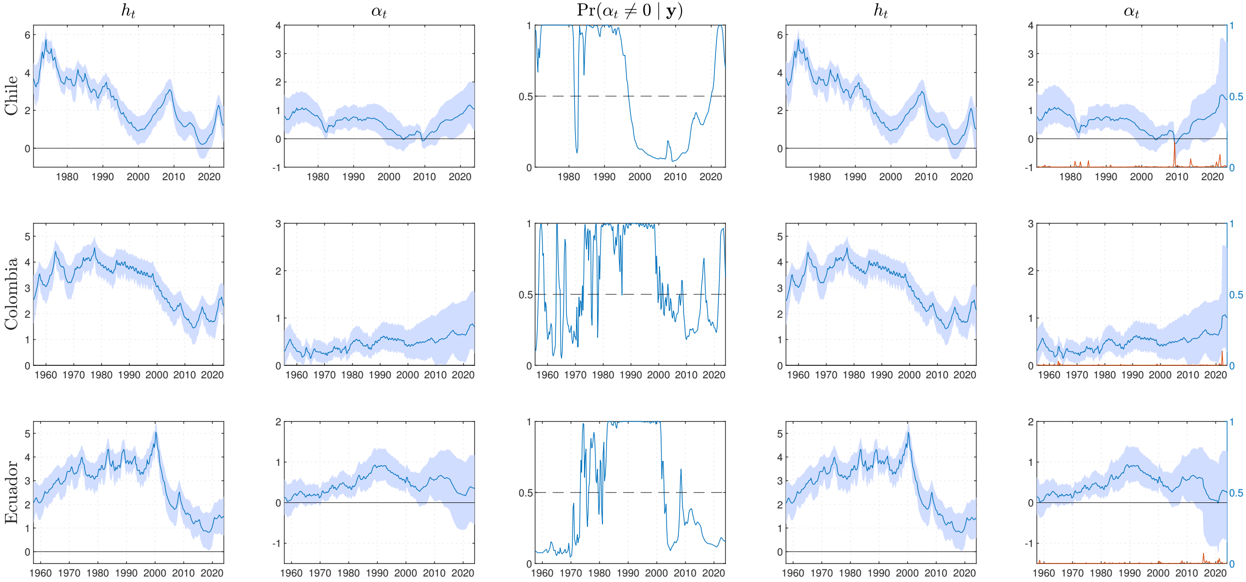

Figure: The Evolution of h_t (1st column) and α_t (2nd column), and the Dynamic Posterior Probabilities of $\alpha_t \neq 0$ (3rd column) for the Restricted Model. The Evolution of h_t (4th column), and α_t and its Probabilities of Break Occurrence $\Pr(K_t = 1|\pi_t) = \pi_t$ (red line) (5th column) for the TVP-SVM-TVMI Model. The blue lines are Median Values. The sky-blue areas are 5- and 95-percentiles Bands.

Dynamics of h_t and α_t for Francia, Italy and Japan

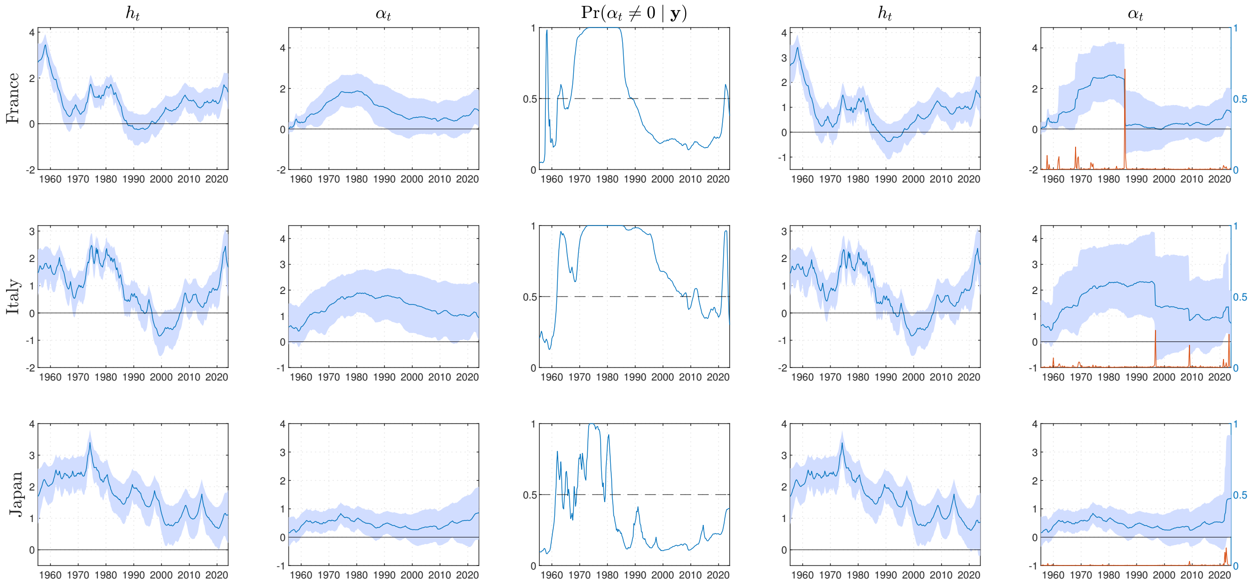

Figure: The Evolution of h_t (1st column) and α_t (2nd column), and the Dynamic Posterior Probabilities of $\alpha_t \neq 0$ (3rd column) for the Restricted Model. The Evolution of h_t (4th column), and α_t and its Probabilities of Break Occurrence $\Pr(K_t = 1|\pi_t) = \pi_t$ (red line) (5th column) for the TVP-SVM-TVMI Model. The blue lines are Median Values. The sky-blue areas are 5- and 95-percentiles Bands.

Dynamics of h_t and α_t for the UK and Uruguay

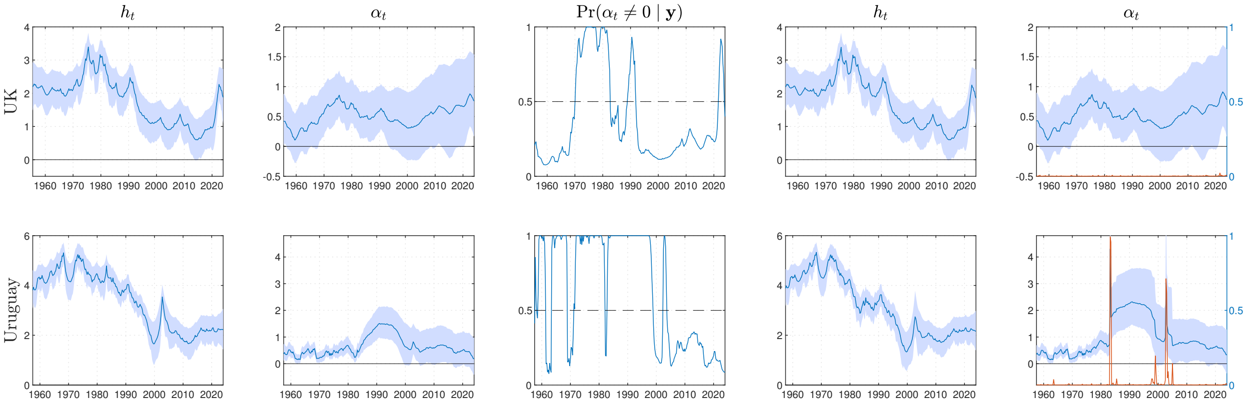

Figure: The Evolution of h_t (1st column) and α_t (2nd column), and the Dynamic Posterior Probabilities of $\alpha_t \neq 0$ (3rd column) for the Restricted Model. The Evolution of h_t (4th column), and α_t and its Probabilities of Break Occurrence $\Pr(K_t = 1|\pi_t) = \pi_t$ (red line) (5th column) for the TVP-SVM-TVMI Model. The blue lines are Median Values. The sky-blue areas are 5- and 95-percentiles Bands.